Time-dependent charge renormalization procedure in QED

Q. Z. Lv,[1,2] J. Betke,[2] Q. Su,[1,2] and R. Grobe[2]

[1]*Beijing National Laboratory for Condensed Matter Physics, Institute of Physics, Chinese Academy of Sciences, Beijing 100190, China*
[2]*Intense Laser Physics Theory Unit and Department of Physics, Illinois State University, Normal, Illinois 61790-4560, USA*
(Received 20 April 2015; published 18 September 2015)

We examine the formation process of the vacuum polarization cloud around a localized charge with space-time resolution permitting us to view the traditional charge renormalization procedure from a dynamical perspective. The asymptotic steady-state charge cloud found in the long-time limit (after the subtraction of a suitable term) matches the distribution predicted by standard perturbative propagator techniques based on Feynman diagrams. This match demonstrates that an alternative (classical-field approximation based) approach can predict the nonlinear properties of the vacuum state. It turns out that some aspects of the polarization dynamics suggest that the vacuum can be viewed as a classical dielectric medium, while other aspects are purely quantum mechanical in nature and cannot be predicted from the Maxwell theory for classical fields.

I. INTRODUCTION

The polarization of the quantum vacuum by a strong electromagnetic field can be related to the displacement of virtual electron-positron pairs. These particles are essential elements for the leading radiative corrections to the propagators of quantum electrodynamics (QED). The theoretical analysis, however, is nontrivial from a conceptual point of view as it involves the procedures of regularization, the introduction of cutoff parameters, and charge renormalization to remove unphysical divergent terms by adjusting the bare coupling parameters of the theory. Diagrammatic perturbative techniques have proven to be powerful tools to describe time-independent properties of various QED systems.

These sophisticated methods can provide highly accurate energies or transition rates. The lowest-order correction to the classical Coulomb potential has become the basis for numerous calculations in nuclear physics and quantum optics and has been verified experimentally with astounding accuracy. As a result of recent developments in laser technology, we can use ultrashort electromagnetic radiation pulses as a new tool to probe also time-dependent properties of the vacuum. This technology might also provide us in the future with sufficiently intense pulses to observe the predicted creation process of electron-position pairs directly from the vacuum [1].

There are numerous conceptually intriguing questions about time-dependent QED processes that have become pertinent due to these technological advances. For example, the formation process of a charge and of its surrounding field of virtual photons is conceptually rather intriguing. How does a created electron (or its Coulomb field) induce a polarization cloud from the vacuum? What are the time scales for this process, and how do they compare with the time it takes to create the particle? Can a steady state be reached? If so, how is this process related to the traditional perturbative charge renormalization procedure? Are there limitations to the simple classical view of the vacuum as a polarizable dielectric medium? A better understanding of these challenges would be quite beneficial in view of the new technological possibilities to probe the temporal aspects of the vacuum with ultrafast and intense electromagnetic fields.

In this paper we examine the time-dependent dynamics of the vacuum polarization process and the related charge renormalization procedure. This will provide us with some insight about how to address some of the challenges raised above. More specifically, we will show that the usual semiclassical approach to the Dirac theory can give us a reliable characterization of the vacuum polarization, in excellent agreement with the Feynman based perturbative method.

II. THEORETICAL FRAMEWORK

From a technical point of view, quantum field theoretical simulations of fundamental QED processes with full space-time resolution are unfortunately conceptually and also computationally demanding due to enormous requirements on CPU time and memory. To make practical progress one can employ the classical-field approximation for the photonic environment [2,3], where the photons associated with the electromagnetic fields are modeled by time-dependent functions rather than second-quantized operators. As with any *ad hoc* approximation, the validity of such an approach needs to be tested to avoid possible misinterpretations. In this approximate framework the Dirac Hamiltonian is given by $h_D = c\boldsymbol{\alpha}[p - e\mathbf{A}(\mathbf{r},t)/c] + mc^2\beta + eV(\mathbf{r},t)$, where $\boldsymbol{\alpha}$ and β are the usual 4×4 Dirac matrices. Here the photon field is represented by classical potentials $\mathbf{A}(\mathbf{r},t)$ and $V(\mathbf{r},t)$ with a given dependence on the position and time. In such an approach, the spatial distribution of the induced charges is obtained from the expectation value of the charge operator in the initial vacuum state $|vac\rangle$,

$$\rho(\mathbf{r},t) \equiv \langle vac|e[\Psi^\dagger(\mathbf{r},t)\Psi(\mathbf{r},t) - \Psi(\mathbf{r},t)\Psi^\dagger(\mathbf{r},t)]/2|vac\rangle. \quad (1)$$

Here the electron-positron field operator $\Psi(\mathbf{r},t)$ is obtained [2,4] in terms of the corresponding fermionic creation and annihilation operators and of all (single-particle) wave functions ϕ that fulfill the Dirac equation $i\hbar\partial\phi/\partial t = h_D\phi$. This expansion of $\Psi(\mathbf{r},t)$ in terms of all single-particle orbitals leads to the final expression for the charge density [3],

$$\rho(\mathbf{r},t) \equiv e\left[\sum_{E+}|\phi_{E+}(\mathbf{r},t)|^2 - \sum_{E-}|\phi_{E-}(\mathbf{r},t)|^2\right]\Big/2, \quad (2)$$

where the first (second) summation extends over all states with an initially positive (negative) energy. In order to get

a computationally feasible model, the simulations below are performed in one spatial direction such that the vector potential can be neglected by choosing an appropriate gauge.

Space-time resolved simulations based on quantum field theory are presently not yet possible in two or three spatial dimensions. However, due to the efficiency of multiprocessor computational platforms simulations are possible in one spatial dimension. It is therefore important to point out that one-dimensional (1D) electrodynamics can have a different behavior at small distances than its three-dimensional (3D) counterpart.

III. VACUUM POLARIZATION

In Fig. 1, we display the numerically obtained solution $\rho(x,t)$ according to Eq. (1) for a charge with the amount $-e$ placed at $x = 0$. This charge does not necessarily represent a physical electron, but more a bare electron, to use the usual language and to reflect the fact that the interaction with the vacuum has not yet occurred. In fact, the presence of this charge is represented in the simulation by an external potential of the form $V(x) = 2\pi k_e e|x|$, where we abbreviate Coulomb's constant as $k_e \equiv 1/(4\pi\varepsilon_0)$, which is related to the vacuum's permittivity ε_0. This is the classical solution obtained from the stationary Maxwell equation $-\partial^2 V(x)/\partial x^2 = 4\pi k_e \rho(x)$, where the associated charge density is $\rho(x) = e\delta(x)$. The associated electric field follows as $E(x) = -\partial V(x)/\partial x = 2\pi k_e qx/|x|$.

The four snapshots show that this particular solution $\rho_{(x,t)}$ increases with time while the shape of the density remains invariant. There are two immediate observations that suggest a purely mathematical character of these particular (numerically fully converged) solutions. The solution grows without any limit and negative charges appear to accumulate around the (originally given) negative charge. While an infinite growth does not necessarily violate energy conservation [5], the accumulation of like charges around the central charge seems unphysical.

In order to better understand and to separate out this divergent part of the Dirac charge density, we have compared it
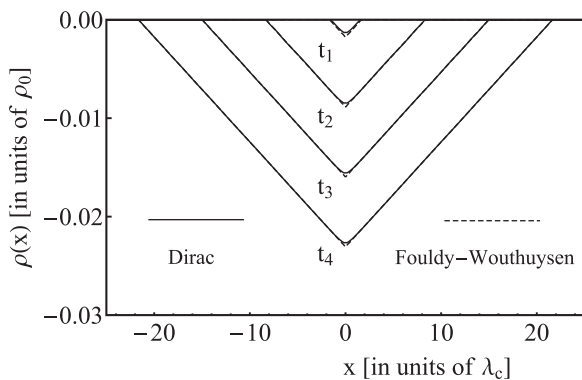

FIG. 1. The time evolution of the solution Eq. (2) (in units of $\rho_0 = 1.6 \times 10^{-19}$ C/m^2) as a function of the position (in units of the Compton wavelength $\lambda_C = 3.86 \times 10^{-13}$ m) under the Dirac and Foldy-Wouthuysen Hamiltonians triggered by a localized charge at $x = 0$. The four moments in time are $t_i = 2.15 \times 10^{-21}$ s $+ (i - 1)4.3 \times 10^{-21}$ s with $i = 1,2,3,4$.

to the corresponding quantity [Eq. (2)] based on the states from the Foldy-Wouthuysen (FW) theory [6]. In the special case of a force-free system ($V = 0$), the corresponding Hamiltonian $\beta\sqrt{m^2c^4 + c^2p^2}$ is equivalent to h_D as it can be obtained by a unitary transformation. To include the potential we examine the Hamiltonian $h_{FW} = \beta\sqrt{m^2c^4 + c^2p^2} + eV(\mathbf{r},t)$. As it is diagonal in spinor-space it cannot account for the relativistic coupling between the positive and negative energy levels. This form permits sometimes an easier interpretation of the dynamics for weakly coupled processes. We note that transitions from the initially occupied negative energy states (Dirac sea) to positive energy eigenstates are usually associated with the creation of electron-positron pairs. In contrast, h_{FW} cannot reproduce those processes that involve the electron-positron pairs such as the polarization. By evolving the field operator under h_{FW}, the corresponding density (denoted by ρ_{FW}) can be obtained according to Eq. (2). Figure 1 shows that h_D and h_{FW} predict nearly identical solutions, except close to $x = 0$.

This match of the two densities illustrates that the (unphysical) infinite growth in Fig. 1 occurs already in the no-coupling limit and therefore cannot correspond to the true vacuum polarization that is intrinsically relativistic. To obtain the physical density, the unphysical FW distribution ρ_{FW} has to be subtracted from the Dirac density ρ_D. As we show below, the polarization potential [7] is proportional to $O(1/c^2)$ and therefore cannot be predicted from h_{FW} whose error is of the same order. It is important to note that the occurrence of mathematical solutions that need to be removed is not unusual for the classical-field approximation. In their pioneering work, Wichmann and Kroll [8] noted first that this approximation leads to the occurrence of diverging mathematical terms for stationary Coulomb systems.

The true origin for these particular solutions is presently not fully understood. One can use some perturbative arguments that suggest that the unphysical contribution to the charge density is associated exclusively with the coupling between states within the upper energy manifold. In other words, we can eliminate these solutions by restricting the permitted couplings of the (free) positive energy states to only those states of the negative energy continuum. In this sense, it is expected that subtracting the FW charge density from the Dirac density eliminates effectively these (for the vacuum polarization process) unphysical transitions within the same energy manifold. It also turns out that these unphysical (converged) solutions do not have any nonrelativistic analog. In fact, the corresponding charge density for the nonrelativistic limit of Eq. (2) (formally obtained by the limit of the speed of light $c \to \infty$), does not lead to any convergent solution at all.

While the properties of these unwanted long-range solutions and possible techniques to eliminate them are understood, their physical origin is not. For example, it could be that these solutions are solely a consequence of the classical-field approximation, where we have neglected the operator character of the photon potential. In the traditional Feynman diagram based approach, which we summarize below, it seems that these unphysical solutions do not occur, or, at least, they were somehow eliminated effectively during the required infinite charge renormalization procedure.
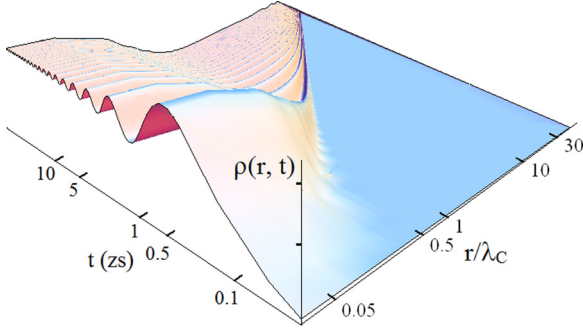
FIG. 2. (Color online) The time evolution of the physical polarized charge density triggered by a point (negative) charge centered at $r \equiv |x| = 0$.
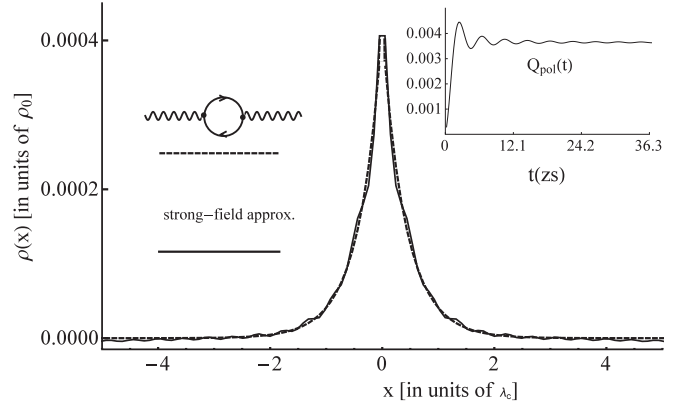

FIG. 3. The comparison between the QED (lowest-order Feynman diagram) charge density and the steady state obtained from the strong-field approximation. The inset graph is the time-averaged total induced charge between $x = -25\lambda_C$ and $25\lambda_C$.

In Fig. 2 we display the time evolution of the physical polarization charge density $\rho \equiv \rho_D - \rho_{\mathrm{FW}}$. In contrast to the data of Fig. 1 (and now fully consistent with our intuition), we observe that a positive charge cloud grows around the central charge. After about 10^{-20} s this density approaches a finite steady state, which has a spatial extension on the order of the Compton wavelength $\lambda_C \equiv \hbar/(mc)$.

The formation of the steady state is accompanied by a combination of small amounts of positive and negative charges that leave the region close to $r = 0$ and propagate outward. The front edge evolves precisely with the speed of light c as is visible by the straight diagonal line in the surface plot. This outgoing portion is transient and damps out in the long-time limit. The period of the damped oscillations is 4×10^{-21} s. This matches exactly $\pi\hbar/(mc^2)$, which is a typical short time scale characteristic of pair creation processes. The amplitude of the oscillations might be related to the sudden turn-on of the charge-vacuum coupling at time $t = 0$.

As mentioned in the introduction time-independent quantities such as the stationary polarization charge density are usually computed in QED based on Feynman diagrams. If we apply this standard technique to our system we have to compute the one-loop correction to the unperturbed photon propagator [9]. If we follow the usual steps (as summarized in the Appendix), including the introduction of the Feynman parameter β and the charge renormalization we obtain the first-order modified photon propagator as

$$D'_{F\mu\nu}(k) = -(4\pi k_e \hbar c^{-1})g_{\mu\nu}/k^2 - 4\pi k_e \hbar c^{-1}$$
$$\times (g_{\mu\nu}k^2 - k_\mu k_\nu)\alpha/k^2[P(k^2) - P(0)]. \quad (3)$$

Here k denotes the two-momentum, k_e is the Coulomb constant in 1D, and α is the corresponding fine structure constant. The term $P(k) - P(0)$ simplifies to $-8\hbar^2 m^{-2}c^{-2}\int_0^1 d\beta\, \beta^2(1-\beta)^2 k^2[m^2c^2\hbar^2 - \beta(1-\beta)k^2]^{-1}$. The inverse Fourier transformation of the first term in Eq. (3) reproduces the usual Coulomb law in one dimension, $V(x) = -2\pi k_e e|x|$, while the second term, $V(x) = 2\pi k_e e\alpha\hbar^3 m^{-3}c^{-3}\int_1^\infty d\tau\, \tau^{-5}\sqrt{\tau^2 - 1}^{-1}\exp(2mc\tau|x|/\hbar)$, gives us the correction due to the vacuum polarization. Invoking the 1D Maxwell equation $\rho(x) = -(4\pi k_e)^{-1}\partial_x^2 V(x)$,

we can compute the associated effective charge density [8],

$$\rho(x) = (e + Q_{\mathrm{pol}})\delta(x) - 2e\alpha\hbar m^{-1}c^{-1}\int_1^\infty d\tau\, \tau^{-3}$$
$$\times \sqrt{\tau^2 - 1}^{-1}\exp(-2mc\tau|x|/), \quad (4)$$

where $Q_{\mathrm{pol}} = 2e\alpha\hbar m^{-2}c^{-2}\int_1^\infty d\tau\, \tau^{-4}\sqrt{\tau^2 - 1}^{-1}$ denotes the total induced charge, which is the negative of the spatial integral over the second term. The renormalized charge $Q_{\mathrm{pol}} + e$ at $x = 0$ ensures that $\int dx\,\rho(x) = e$, as required.

In Fig. 3 we compare the induced charge distributions obtained from the Feynman method and from the classical-field approximation. The agreement is superb. The small oscillatory structures are remnants of the time evolution and vanish in the long-time limit. The match is an encouraging confirmation that the classical-field approximation, which is usually employed for superstrong fields, is valid to predict the vacuum polarization process.

The total induced charge close to $x = 0$ approaches a constant value for the dynamical process, which can be computed as $Q_{\mathrm{pol}}(t) = 1/t\int_0^t dt'\int dx\,\rho_{\mathrm{pol}}(x,t')$ to average locally over the oscillations. It is shown in the inset of Fig. 3.

Interestingly, the total amount of the induced charge that originates close to $r = 0$ is positive, but this does not violate charge conservation, as the total charge operator commutes with the Dirac Hamiltonian. This conservation law should not be misinterpreted and be applied locally to the vicinity of $r = 0$. It is a global quantity. The missing equal portion of the accompanying induced negative charges is generated at the boundaries of our numerical box (not shown in the figure) where the potential behaves as if there was effectively a second (oppositely charged) mirror charge.

While the vacuum's polarization is a quantum mechanical process, a comparison with the polarization of a classical dielectric medium could help us to better understand this. As classical microscopic dipoles realign themselves in an electric field (for instance, between two charged parallel plates), also here the induced charges build up simultaneously at both edges of the capacitor, in full analogy to our situation where the total charge is also conserved.

In contrast to the standard mathematical charge renormalization procedure where the amount of the bare charge is dictated by the required (measured) long distance behavior of the Coulomb force law, the time-dependent simulation started with a given central negative charge, which then induced the positive charge cloud around it. As a result, the central charge becomes naturally screened such that the total effective charge observed from a large distance would be less than the original amount. In other words, the dynamical polarization process lowers the total charge. This is in contrast to the mathematical renormalization procedure where the original value of the bare charge has to be artificially readjusted (renormalized) after the fact to become consistent with the required total charge observed from a distance. In this sense the mathematical renormalization procedure based on a readjustment of the central charge can reproduce the steady-state distribution that is obtained from the dynamical polarization process starting from an isolated charge. One could therefore expect that there might be other nonperturbative quantum-field-theoretical methods available for which an initial unrenormalized charge state would naturally relax into the fully polarized state. This could be analogous to the standard imaginary time integration technique routinely used to determine ground states.

The classical field approach might suggest that the quantum vacuum can be viewed as a simple classical dielectric medium that can be polarized by an external force field. To examine if this conjectured analogy really holds and the electric field is solely responsible for the polarization, we have modified the geometry of the original charge configuration. Instead of the point charge studied above, we compute the polarization charge density for two initially charged plane parallel capacitor plates. It is well known that if the two plates are infinitely extended and oppositely charged, the two electric fields associated with each plate cancel exactly out and there is no classical electric field in the two regions outside the plates. If this capacitor were inserted into a classical dielectric medium, we would not expect any polarization charges outside the plates.

In Fig. 4 we examine the corresponding induced density from the vacuum. For simplicity we have assumed that the two plates are infinitesimally thin. Again, the long-time limit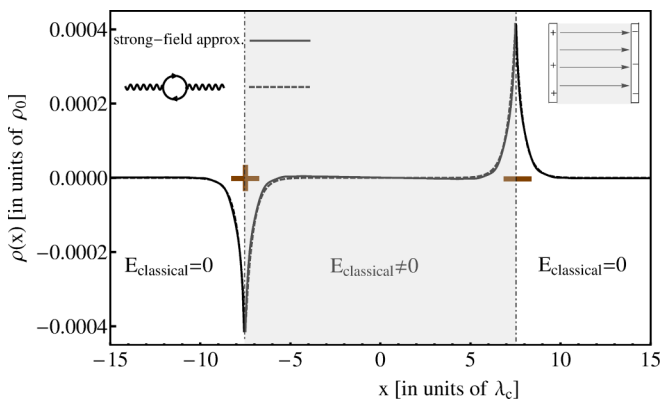 matches the charge density predicted by the lowest-order Feynman diagram method. We observe that there are induced charges from the vacuum even in the two regions where the (classical) electric field is zero. This is in contrast to the absence of any polarization as predicted by the Maxwell equations for a classically dielectric medium. Apparently charges can be induced from the vacuum even in "classically forbidden" regions. While there are commonalities between the dynamical response of the vacuum and a dielectric medium, this finding suggests that it is not trivial to assign a dielectric permeability to the quantum vacuum. The induced charges have also a detectable impact on the total attractive force between the plates, similar to the Casimir force.

IV. SUMMARY

In conclusion, we have shown that the classical-field approximation can be directly connected with the traditional Feynman diagram based approach for the vacuum polarization if appropriate mathematical solutions (related to the Foldy-Wouthuysen theory) are subtracted from the density obtained from the Dirac Hamiltonian. This has two consequences. First, it leads to the observation that the mathematical charge renormalization procedure can be identified as the long-time limit of a dynamical relaxation process. This opens the possibility to derive alternative relaxation-based techniques to the usual renormalization procedures. Second, it has a direct implication for self-consistent solution techniques to the coupled Maxwell-Dirac equation, where the current and charge densities act as source terms. To mention an important example, these coupled equations are the basis for examining the interfermionic interactions of the strong-field induced electron-positron pair creation process, which has been studied so far [10,11] exclusively in the framework of the strong-field approximation. Here it is important to note that reliable results can only be obtained if in each step of the coupled dynamics the corresponding mathematical solutions are removed from the space-time–dependent current density. We will provide more details on how this can be accomplished in a separate work.

APPENDIX

Here we summarize briefly the usual derivation for the vacuum's polarization charge density of Eq. (4). We denote with x the two-vector $x^\mu \equiv (ct,x)$ and with k the two-vector $k^\mu \equiv (\omega/c,k_x)$. We use the same polarization tensor as in 3D calculations, except that we replace $\int d^4k/(2\pi)^4$ by

FIG. 4. (Color online) The induced polarization density for two infinitely extended parallel charged plates.

$\int d^2 k/(2\pi)^2$. The corresponding diagram exhibits also a logarithmic divergence; however, by using dimensional regularization it turns out that this contribution in fact cancels such that the polarization tensor is finite in 1D. As a result it can be directly simplified to $\Pi_{\sigma\lambda}(k) \equiv \kappa_b^2 \hbar^{-2}(4\pi)^{-1}(g_{\sigma\lambda}k^2 - k_\sigma k_\lambda)P(k^2)$, with

$$P(k^2) = -8 \int_0^1 d\beta\, \beta(1-\beta)[m^2 c^2 \hbar^{-2} - \beta(1-\beta)k^2]^{-1}. \tag{A1}$$

As the result, the propagator takes the form

$$\begin{aligned} D'_{F\mu\nu}(k) = &-(4\pi k_e \hbar c^{-1})k^{-2}g_{\mu\nu} - \kappa_b^2 \hbar^{-2}(4\pi)^{-1} \\ &\times P(k^2)(g_{\mu\nu}k^2 - k_\mu k_\nu)(4\pi k_e \hbar c^{-1})^2 k^{-4}. \end{aligned} \tag{A2}$$

Next we convert the modified photon propagator into the potential for a bare charge κ_b centered at $x = 0$, according to $j^\nu(x) = c\kappa_b \delta^{\nu 0}\delta(x)$. In Fourier space, we obtain the zeroth component of the potential:

$$\begin{aligned} A'_0(k) = &\kappa_b(4\pi k_e c^{-1})k_x^{-2}2\pi\delta(k_0) \\ &+ \kappa_b^3 k_e(c\hbar)^{-1}P(-k_x^2)(4\pi k_e c^{-1})k_x^{-2}2\pi\delta(k_0). \end{aligned} \tag{A3}$$

Similarly as in the corresponding derivation of the 3D world, we need to find (renormalize) the (unknown) value of the coupling κ_b. In contrast to the real 3D world, where we have an observable value of the charge of the underlying fundamental particle (positron), there are obviously no experimental reference measurements in the mathematical 1D world. We denote with e the physical charge of the corresponding ficticious elementary particle in 1D.

The corresponding true 1D potential should behave as $A_0^{\rm ref}(x) \to c^{-1}e 2\pi k_e|x|$ for large distances. In Fourier space, this corresponds to $A_0^{\rm ref}(k) \to e 4\pi k_e c^{-1}/k_x^2$. So equating Eq. (A3) and $A_0^{\rm ref}(k)$ we obtain

$$\begin{aligned} 4\pi k_e c^{-1}e/k_x^2 = &\kappa_b 4\pi k_e c^{-1}k_x^{-2} + \kappa_b^3 k_e(c\hbar)^{-1} \\ &\times P(-k_x^2)(4\pi k_e c^{-1})k_x^{-2}, \end{aligned} \tag{A4}$$

where the factor $2\pi\delta(k_0)$ was canceled on both sides and k^2 was replaced by $-k_x^2$. This equation simplifies for $k_x \to 0$ to

$$e = \kappa_b + \kappa_b^3 k_e(\hbar c)^{-1}P(0). \tag{A5}$$

If we solve this equation for κ_b as a function of e we obtain again one real and two complex solutions. We assume that we can expand the real solution to first order in the unitless parameter $k_e(\hbar c)^{-1}e^2 P(0)$, noting, however, that (in contrast to the 3D theory) $P(0)$ is finite [12]. We define $k_e e^2/(\hbar c) \equiv \alpha$, which introduces α as an effective fine structure constant in 1D. The final solution of Eq. (A5) is

$$\kappa_b = e - \alpha P(0)e + O((\alpha P(0))^2). \tag{A6}$$

If we replace this expression for the coupling κ_b in terms of the elementary charge e back into Eq. (A3), we obtain the final result for the potential of a 1D elementary charge e (and the 1D fine structure constant α),

$$A'_0(k) = \{1 + \alpha[P(-k_x^2) - P(0)]\}e k_x^{-2}4\pi c^{-1}k_e\, 2\pi\delta(k_0). \tag{A7}$$

The finite term $P(k) - P(0)$ simplifies to

$$\begin{aligned} P(k) - P(0) = &-8\hbar^2 m^{-2}c^{-2}\int_0^1 d\beta\, \beta^2(1-\beta)^2 k^2 \\ &\times [m^2 c^2 \hbar^{-2} - \beta(1-\beta)k^2]^{-1}. \end{aligned} \tag{A8}$$

In position representation, the zeroth component of the potential, $V = cA'_0$, for the charge e centered at $x = 0$ becomes

$$\begin{aligned} V(x) = &-2\pi k_e e|x| + 2\pi k_e e\alpha\hbar^3 m^{-3}c^{-3}\int_1^\infty d\tau\, \tau^{-5} \\ &\times \sqrt{\tau^2 - 1}^{-1}\exp(-2mc\tau|x|/\hbar). \end{aligned} \tag{A9}$$

This result can be effectively interpreted as being a polarization charge density due to the vacuum polarization correction, which can be determined from the classical Maxwell equation as $\rho(x) = -(4\pi k_e)^{-1}\partial_x^2 V(x)$. We obtain Eq. (4) of the main text:

$$\begin{aligned} \rho(x) = &(e + Q_{\rm pol})\delta(x) - 2e\alpha\hbar m^{-1}c^{-1}\int_1^\infty d\tau\, \tau^{-3} \\ &\times \sqrt{\tau^2 - 1}^{-1}\exp(-2mc\tau|x|/\hbar), \end{aligned} \tag{A10}$$

where $Q_{\rm pol} \equiv 2e\alpha\hbar^2 m^{-2}c^{-2}\int_1^\infty d\tau\, \tau^{-4}\sqrt{\tau^2 - 1}^{-1}$ denotes the induced charge.

[1] For a recent review, see, e.g., A. Di Piazza, C. Müller, K. Z. Hatsagortsyan, and C. H. Keitel, Rev. Mod. Phys. **84**, 1177 (2012).

[2] W. Greiner, B. Müller, and J. Rafelski, *Quantum Electrodynamics of Strong Fields* (Springer Verlag, Berlin, 1985).

[3] H. K. Avetissian, *Relativistic Nonlinear Electrodynamics* (Springer, New York, 2006).

[4] T. Cheng, Q. Su, and R. Grobe, Contemp. Phys. **51**, 315 (2010).

[5] A. T. Steinacher, J. Betke, S. Ahrens, Q. Su, and R. Grobe, Phys. Rev. A **89**, 062106 (2014).

[6] L. L. Foldy and S. A. Wouthuysen, Phys. Rev. **78**, 29 (1950).

[7] E. A. Uehling, Phys. Rev. **48**, 55 (1935).

[8] E. H. Wichmann and N. H. Kroll, Phys. Rev. **101**, 843 (1956).

[9] For a review, see, e.g., M. D. Schwartz, *Quantum Field Theory and the Standard Model* (Cambridge University Press, Cambridge, UK, 2013).

[10] F. Hebenstreit, J. Berges, and D. Gelfand, Phys. Rev. Lett. **111**, 201601 (2013).

[11] A. T. Steinacher, R. Wagner, Q. Su, and R. Grobe, Phys. Rev. A **89**, 032119 (2014).

[12] Y. Kluger, J. M. Eisenberg, and B. Svetitsky, Phys. Rev. D **45**, 4659 (1992).